RSC Advances

ROYAL SOCIETY OF CHEMISTRY

www.rsc.org/advances

A graphic abstract

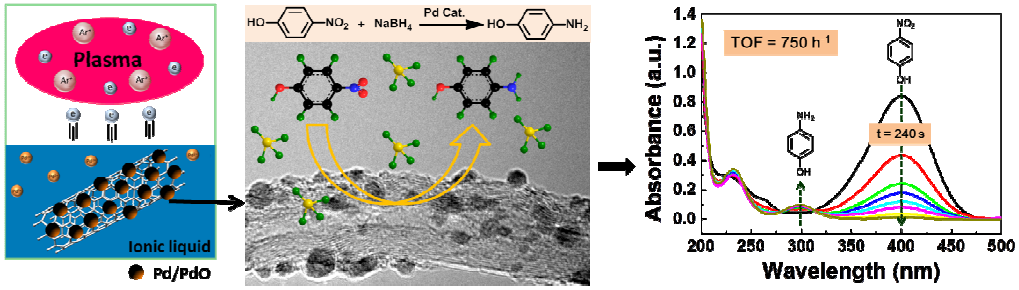

In this work, Pd/PdO nanoparticles supported on oxidized multi-walled carbon nanotubes (OCNTs) catalyst is first time prepared by a one-pot gas-liquid interfacial plasma (GLIP) method with the precursor $Pd(NO_3)_2 \cdot 2H_2O$. Our results demonstrate that the presence of PdO nanoparticles can significantly enhance the catalytic performance of Pd catalyst for the reduction of 4-nitrophenol (4-NP).

Journal Name

RSCPublishing

ARTICLE

PdO Nanoparticles Enhancing the Catalytic Activity of Pd/Carbon Nanotubes for 4-Nitrophenol Reduction

Cite this: DOI: 10.1039/x0xx00000x

Received 00th January 2012,
Accepted 00th January 2012

DOI: 10.1039/x0xx00000x

www.rsc.org/

Chunxia Wang,[a‡] Fan Yang,[b‡*] Wang Yang,[b] Liang Ren,[b] Yunhan Zhang,[b] Xilai Jia,[b] Liqiang Zhang,[b] and Yongfeng Li[b*]

In this work, we demonstrate that the presence of PdO nanoparticles can significantly enhance the catalytic performance of Pd catalyst for the reduction of 4-nitrophenol (4-NP). Heterogeneous Pd/PdO nanoparticles supported on oxidized multi-walled carbon nanotubes (OCNTs) catalyst is prepared by a one-pot gas-liquid interfacial plasma (GLIP) method with the precursor $Pd(NO_3)_2 \cdot 2H_2O$. The Pd/PdO catalysts with uniform size distribution exhibit remarkable catalytic activity during the reduction of 4-NP to 4-aminophenol (4-AP) in neat water at room temperature. The turnover frequency (TOF) value is up to 750 h^{-1}, which shows much higher catalytic activity than single Pd nanoparticles supported on OCNTs. Our results indicate that the Pd/PdO catalyst can be readily recovered and reused for 10 times.

Introduction

Metallic nanoparticles have attracted much more attention in recent years due to their catalytic properties and potential applications, which may differ considerably from the bulk metal.[1-3] Among the metallic nanoparticles catalysts, Pd nanoparticles are the most widely used in catalysis, such as Suzuki reactions in both aqueous and non-aqueous solvents,[4] α-alkylation of ketones and ring-opening alkylation of cyclic 1,3-diketones with primary alcohols,[5] semi-hydrogenation of phenylacetylene,[6] hydrogenation of olefins[7] and unsaturated alcohols,[8] hydrodechlorination of chloroorganic compounds,[9] etc.[10] Moreover, PdO nanoparticles, as another type of Pd nanoparticles, are found to be very good catalysts for the aerobic oxidation of benzyl alcohol in water.[11] Supported PdO catalysts bring about the transformation of CH_4,[12] and charcoal-supported palladium oxide nanoparticles are used to catalyze the Sonogashira reactions,[13] what's more, PdO/TiO_2 heterostructured nanobelts are used to enhance photocatalytic activity.[14] Meanwhile, there exists some evidence showing that the Pd/PdO nanoparticles can enhance the catalytic activity in comparison with Pd nanoparticles in catalysis,[15,16] since the complex electron interaction between the Pd and PdO component,[17] and the reaction activity on the metal surface is not as high as at the phase boundary of Pd and PdO component in methane dissociation.[18] Therefore, it is interesting and meaningful to develop the high efficient Pd/PdO catalysts.

Due to the high surface energy of free nanoparticles tend to aggregate, it is difficult to handle in catalytic applications. Many inert solid materials such as mesoporous solids (MCM-41, SBA-15 or related mesoporous silicas),[19-21] polymers,[22,23] metal oxides[24-26] and metal-organic framework (MOF)[27-29] have been successfully applied to stabilize the particles. However, most of these supports are synthetic materials which require laborious and time-consuming efforts for their synthesis as well as surface functionalization to preserve high reactivity of catalyst. The carbon nanotubes (CNTs) have been normally used as a material support for the dispersion and stabilization of metal nanoparticles due to their large chemically active surface, unique physical properties, inherent size, hollow geometry and stability at high temperatures.[30] Moreover, CNTs have been mass-produced by a CVD method.[31] Therefore, the development of the nanoparticles (NPs) and CNTs hybrid materials as high reactivity catalyst is highly required.

To effectively synthesize the Pd nanoparticles, several synthetic strategies including electrodeposition, electroless deposition, arc-discharge in solution, sonochemical method, microwave-assisted, and chemical reduction in supercritical CO_2 solution have been devel-oped.[23-27] Whereas, the PdO

[a]*Beijing National Laboratory for Molecular Sciences, Key Laboratory of Analytical Chemistry for Living Biosystems, Institute of Chemistry, the Chinese Academy of Science, Beijing 100190, China*

[b]*State Key Laboratory of Heavy Oil Processing, China University of Petroleum, Beijing, Changping 102249, China. Phone/Fax: +86-010-89739028. E-mail: yangfan@cup.edu.cn, yfli@cup.edu.cn.*

‡ These authors contributed equally.

† Electronic Supplementary Information (ESI) available: materials, experimental setup, and UV-vis spectra.

nanoparticles are usually synthesized by calcinating Pd nanoparticles in air, and by stirring the Pd salt under the oxidation conditions.[32-36] However, the synthesis of Pd/PdO nanoparticles is still challenging at the present time, for the reason that the formation of Pd nanoparticles need reduction conditions, whereas the formation of PdO nanoparticles need oxidation conditions. Therefore, successfully solving the above contradiction is the key to the synthesis of the Pd/PdO nanoparticles. Until now, the most common method to synthesize the Pd/PdO nanoparticles is calcination treatment of the Pd nanoparticles, however, the stabilizer or surfactant is usually needed to avoid the over oxidation or aggregation of the particles.[37-40] As is known to all, the stabilizer and surfactant are not usually indispensable for catalysis. Therefore, development of a facile method to synthesize the Pd/PdO nanoparticles is of great significance.

Herein, we report for the first time that the controllable synthesis of Pd/PdO and Pd nanoparticles functionalized oxidized CNTs (Pd/PdO/OCNTs and Pd/OCNTs) by the GLIP method under low argon pressure with using different Pd salt precursors. Recently, researchers focused on the fabrication of metal nanoparticles by using the GLIP method,[41,42] which show unique properties of high process rate, preparation of nanomaterials in large scale, avoiding the use of toxic stabilizers and reducing agents, ambient reaction temperature, and no need to stir during the nanoparticle formation process. All the above advantages provide a facile and low-cost alternative way to prepare Pd nanoparticles.[43-45] More importantly, it can provide weaker reduction conditions than $NaBH_4$ and hydrazine hydrate reduction systems, and the emission of argon is produced along with glow.[46,47] Therefore, we treat the $Pd(NO_3)_2{\cdot}2H_2O$ in GLIP condition so that the $Pd(NO_3)_2{\cdot}2H_2O$ can be reduced to Pd nanoparticles along with decomposing to PdO by the glow, and the formed PdO nanoparticles cannot be reduced by the glow system, which provides an efficient pathway to synthesize the Pd/PdO nanoparticles. Furthermore, the catalytic performance of the resultant hybrid materials is assessed by studying the reduction of 4-NP reaction, and the catalytic activity of Pd/PdO/OCNTs is better than Pd/OCNTs which could be ascribed to the existence of PdO active species. To the best of our knowledge, we report for the first time that the PdO species in the presence of Pd nanoparticles can enhance the reactivity for reduction of 4-NP.

Experimental

General information

All chemicals and reagents were purchased from commercial suppliers without further purification unless otherwise stated. The transmission electron microscopy (TEM, Tecnai G2, F20) combined with an energy dispersive X-ray spectroscopy (EDS) at an acceleration voltage of 200 kV was used to measure the size, morphology, size distribution and element content of Pd catalysts. X-ray diffraction (XRD, Bruker D8 Advance Germany) was applied to characterize the crystal structure of the hybrid materials, and the data was collected on a Shimadzu XD-3A diffractometer using Cu Kα radiation. The X-ray photoelectron spectroscopy (XPS, Thermo Fisher K-Alpha American with an Al K α X-ray source) was used to measure the elemental composition of samples. The amounts of Pd were determined by an inductively coupled plasma optical emission spectrometer (ICP-OES). UV-vis absorption spectra of the samples were recorded at room temperature on a TU-1900 apparatus.

Fabrication of the OCNTs

The CNTs used in our experiments were purchased from Beijing Cnano Technology Limited (Purity: > 95%, average length: 10 μm, average external diameter: 11 nm). The OCNTs were prepared by oxidation of purified CNTs (1 g) with 100 ml cooled piranha solutions (4:1, vol/vol 96% H_2SO_4/30% H_2O_2) at 25 ^oC for 100 min. The resulting mixture was diluted with ice water. After that, the obtained suspension was centrifuged at 4000 rpm for 10 min and washed with distilled water for several times until the pH of the mixture reached 7. Finally, the precipitate obtained was dried in a vacuum oven at 60 ^oC for 12 h before use.

Fabrication of the Pd/PdO/OCNTs and Pd/OCNTs hybrid materials

The Pd/PdO/OCNTs catalysts were prepared by a GLIP method with $Pd(NO_3)_2{\cdot}2H_2O$ and OCNTs at room temperature for 10 min, and the obtained materials were called Pd-1. The glow plasma was generated between the top flat stainless steel (SUS) and the bottom ionic liquid electrode. Argon gas was introduced and used as the plasma-forming gas. The voltage between two electrodes V_{DC} = 200-230 V was applied to a stainless steel electrode in gas phase for the generation of an argon plasma, where the discharge current was fixed to 1 mA and the Argon gas was introduced up to a pressure of 140 Pa. 12.8 mg of $Pd(NO_3)_2{\cdot}2H_2O$ was dissolved into 1 mL ionic liquid 1-butyl-3-methylimidazolium tetrafluoroborate ([bmim]BF_4), 48 mg OCNTs and the obtained $Pd(NO_3)_2{\cdot}2H_2O$ in the ionic liquid solution were added to the stainless steel reactor and incubated for 15 min. For the formation of Pd/PdO nanoparticles, electrons were irradiated toward the ionic liquid for 10 min, and then the mixture was sonicated in ethanol to remove the excess impurities and extracted from the ionic liquid by a centrifuge process. The Pd/OCNTs hybrid materials were prepared by using the same procedure with different Pd salt precursors including $Pd(OAc)_2$, K_2PdCl_4 as well as $PdCl_2$, and the corresponding materials depicted in this study are defined as [Pd-n], (n = 2, 3, 4).

Fabrication of PdO/OCNTs hybrid materials

PdO/OCNTs was synthesised according to the reported method.[48] OCNTs (50 mg) was dispersed in 100 mL 50 vol% methanol-water. After sonication for half an hour in an ultrasonic bath, the flask was placed on a magnetic stirrer. 20 mL of 14 mg $Pd(NO_3)_2{\cdot}2H_2O$ was added dropwise for 10 min

to produce PdO/OCNTs. The mixture was stirred at room temperature for an hour and then separated by centrifugation. The sample was obtained by washing repeatedly with deionized water, and the corresponding materials depicted in this study are defined as Pd-5.

Catalytic reduction of 4-NP in quartz cuvette (method A)

The Pd-1 catalyst, corresponding to a percentage of Pd of 2 mmol% with respect to 4-NP was used, and 1.5 mL 4-NP (0.1 $mmolL^{-1}$) and 1.5 mL freshly prepared aqueous solution $NaBH_4$ (10 $mmolL^{-1}$) were mixed together in a quartz cuvette. Subsequently, 34 μL Pd-1 catalysts in stock solution (1.0 mg Pd-1 catalyst dispersed in 1 mL miliQ-water) are added to the above mixture by gentle shaking. UV-vis absorption spectroscopy of samples was recorded to monitor the change in the reaction mixture every 70 s over the range from 200 to 500 nm at room temperature. Unless otherwise mentioned, all experiments in quartz cuvette for the conversion of 4-NP to 4-AP with the other Pd-n and Pd-5 were carried out under the same conditions.

Catalytic reduction of 4-NP in micro-reaction vial (method B)

In a typical catalysis reaction in micro-reaction vial, Pd-1 catalyst, corresponding to a percentage of Pd of 2 mmol% with respect to 4-NP was used, and 7.0 mg 4-NP (0.05 mmol) and 1.1 mg Pd-1 catalyst were mixed together in 1 mL miliQ-water then stirred for 1 min in order to mix thoroughly in a micro-reaction vial. Subsequently, 189 mg $NaBH_4$ (5 mmol) in 3 mL miliQ-water was added into the above solution by vigorous magnetic stirring. After that, 12 μL of the reaction mixture was collected and diluted to 3 mL with miliQ-water for UV-vis measurement every 30 s. UV-vis absorption spectra were recorded to monitor the change in the reaction mixture over the range from 200 to 500 nm at room temperature. The catalytic reaction for the conversion of 4-NP to 4-AP performed by using the other three Pd-n catalysts were carried out under the same conditions. Each run of the recycling Pd-1 was carried out under the same conditions, and the reusing Pd-1 was recovered by filtering off the solution of the previous run after reaction has been completed.

Results and discussion

The Pd/PdO catalyst was prepared by a GLIP method using $Pd(NO_3)_2{\cdot}2H_2O$ as a precursor, which is defined as Pd-1. The experimental setup used for the synthesis of catalysts has been reported in our previous work.[43-45] The schematic illustration of plasma system was shown in Fig. S1. In order to compare the effect of different Pd salt precursors for synthesis of the Pd catalysts, several kinds of Pd nanoparticle decorated OCNTs catalysts with different Pd salt precursor ($Pd(OAc)_2$, K_2PdCl_4, $PdCl_2$) are prepared by the above mentioned method, and the corresponding materials are called Pd-n (n = 2, 3, 4).

The morphology of Pd-n has been examined by TEM, as shown in Fig. S2. The distribution histograms of the diameter are summarized in Fig. S3, and the representative TEM images of Pd-1 are shown in Fig. 1a and 1b. These results demonstrate that all the synthesized Pd-n catalysts exhibit uniform morphologies, and the average particle diameters of Pd-1, Pd-2, Pd-3 and Pd-4 are 3.5, 3.7, 8.6 and 3.6 nm, respectively. The Pd loading content of Pd-1, Pd-2, Pd-3 and Pd-4 are 9.5, 10.0, 5.1 and 8.5 wt.%, respectively, as summarized in Table S1. It is found that the particle size of Pd nanoparticles except for Pd-3 is below 4 nm. The large particle size of Pd-3 is probably due to the introduction of potassium ions which leads to the size increase of Pd nanoparticles. In order to check the crystallinity of the synthesized Pd catalysts, a relatively large Pd nanoparticle of Pd-1 has been examined by the high-resolution TEM (HRTEM), as seen in Fig. 1c，where the interfinger distances of 0.225, 0.195 and 0.340 nm are found, corresponding to the (111), (200) lattice plane of the face-centred-cubic (fcc) palladium and shells separation of CNTs, respectively.

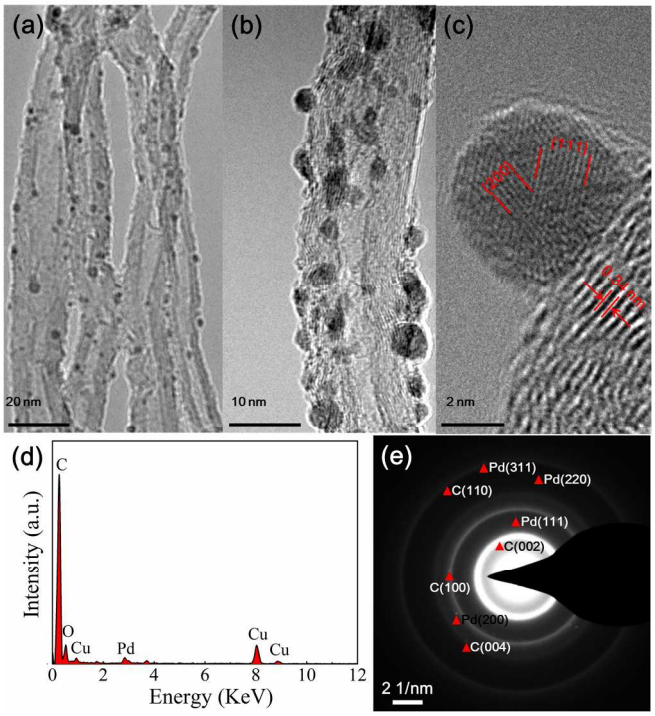

Fig. 1. A TEM image of Pd-1 (a) and (b), HRTEM image of Pd-1 (c), EDX spectrum (d) and SAED image (e) of Pd-1.

In addition, EDX spectra of Pd-1 is indicated in Fig. 1d, in which elements C and O origin from OCNTs, and Cu element is attributed to Cu grid of TEM, Pd element is considered to be originated from Pd nanoparticles. What's more, SAED pattern provides quick and easy crystal orientation information of the obtained Pd-1, as shown in Fig. 1e. The lattice spacing measured from the diffraction rings were 0.35, 0.23, 0.21, 0.20, 0.17, 0.13, 0.12 and 0.11 nm, corresponding to reflections C(002), Pd(111), C(100), Pd(200), C(004), Pd(220), C(110) and Pd(311), respectively. Furthermore, XRD spectra of Pd-n is depicted in Fig. 2 which shows the diffraction peaks at 25.9°, 40.2°, 42.6°, 46.5°, 53.3°, 68.1° and 82.0°, corresponding to C(002), Pd(111), C(100), Pd(200), C(004), Pd(220) and

Pd(311), respectively. The lattice spacing of the C and Pd is calculated by the Bragg's formula, which is consistent with the measured results from the SAED pattern (Fig. 1e). These results have confirmed that the Pd-n possess a face-centered crystalline structure. The XRD image of Pd-1 also shows one extra peak at 33.8° which can be attributed to the reflection of PdO(101). In order to verify the presence of both Pd and PdO in Pd-1, we also synthesized the Pd-5, and the TEM image, XPS spectra and XRD of Pd-5 are shown in Figs. S4 and S5. The XRD pattern of Pd-5 (Fig. S5d) indicates the characteristic peak at 33.8° is attributed to the reflection of PdO (101), which is consistent with the XRD results of Pd-1.

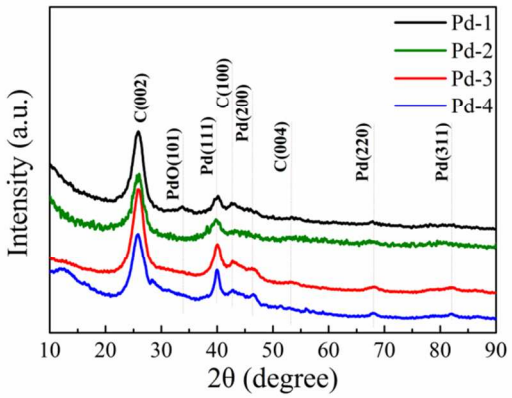

Fig. 2. The XRD patterns of Pd-1 (black curve), Pd-2 (olive curve), Pd-3 (red curve) and Pd-4 (blue curve).

In order to certify the chemical element states of the Pd catalysts, XPS, a powerful technique for the investigation of CNT-based hybrid materials was used to confirm the component of catalysts. Wide XPS scan from Pd-n (Fig. 3a) shows the presence of Pd, C and O derived from OCNTs, which is in agreement with the EDX measurement. The peaks at 284.08 and 532.08 eV clearly indicate that the chemical components are C1s and O1s, respectively. A small peak corresponding to Pd3p is observed at 562.08 eV. Fig. 3b shows the enlarged XPS scan of Pd3d, the two peaks of Pd-2, Pd-3, Pd-4 for Pd 3d appeared at 336.32 and 341.37 can be assigned to $Pd3d_{5/2}$ and $Pd3d_{3/2}$, which indicates the presence of Pd metal (Pd^0) in the catalyst. By comparison, XPS-peak-imitating analysis of Pd-1 shows two peaks for $Pd3d_{5/2}$ and $Pd3d_{3/2}$ which are split into two types of Pd electronic states (Pd and PdO) centred at 334.78, 337.48, 340.18 and 342.58 eV, as shown in Fig. 3c. Moreover, the XPS spectra of Pd-5 indicates that we have successful synthesized the PdO/OCNTs with a little amount of Pd^0, as shown in Figs. S5a and b. Fig. S5c shows the XPS spectra of Pd-5 and Pd-n, indicating clearly that the PdO nanoparticles are present in Pd-1 and absent from Pd-2, Pd-3 and Pd-4. Also, the O1s XPS can be divided into four components, including a PdO bond at 530.08 eV, a C=O bond at 531.18 eV, a O-H bond at 532.28 eV and a C-O bond at 533.68 eV (Fig. 3d). What's more, the spectra of C1s XPS is split into four functional groups, including a C sp2 bond at 284.3 eV, a C-C bond at 285.08 eV, a C=O bond at 286.68 eV, and a C-C=O bond at 289.68 eV, as indicated in Fig. S6. These XPS results suggest that the Pd-1 consists of both Pd and PdO active species,[39] which is probably owing to using $Pd(NO_3)_2 \cdot 2H_2O$ as Pd precursor. The synergistic effect between Pd and PdO may play an important role in the high activity of catalyst.

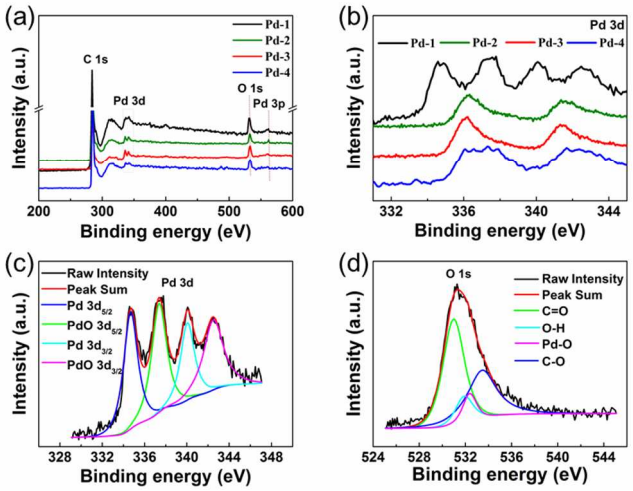

Fig. 3. XPS spectra of Pd-n (a), (b); high-resolution XPS spectra of Pd-1, Pd3d (c) and O1s (d).

As a type of arene, 4-nitrophenol (4-NP) is highly toxic and has detrimental effect on human health and environment as toxic and mutagenic substances.[49] On the other hand, aside from being an important intermediate in the preparation of several analgesic and antipyretic drugs, 4-AP has also been applied as photograph developer, corrosion inhibitor, anti-corrosion lubricant and hair-dyeing agent.[50] Therefore, we evaluate the catalytic activity of as-prepared Pd-n by reducing 4-NP to 4-AP, which is an ideal reaction for characterizing the activity of Pd-n catalysts. 4-NP is pale yellow in aqueous solution which shows plasmon bond absorption centred around 317 nm, as shown in Fig. 4a curve B. After the addition of $NaBH_4$, the color of the solution changes to yellow, which means that phenolate ions have been produced, as a result, a new absorption band appears at 400 nm, as shown in Fig. 4a curve C. Although $NaBH_4$ is well known as a strong reductant, the reduction of 4-NP is quite slow (Fig. 4a curve D), even though OCNTs were introduced into the above reaction solution (Fig. 4a curve E), the reaction rate does not show any considerable progress. Thus, catalysts are usually needed to accelerate the conversion rate of 4-NP to 4-AP.

Initially, the Pd-n are used as catalysts, and their catalytic performance is evaluated by using model reaction of the reduction of 4-NP to 4-AP in aqueous solution at room temperature in quartz cuvette (method A). The evolution of UV-vis spectra with reaction time for the reduction of 4-NP to 4-AP by using different catalysts is monitored, as shown in Fig. S7. The intensity of the absorption band at 400 nm decreases gradually with time increasing. At the same time, a new

absorption band at 300 nm appears as shoulders, being ascribed to the formation of 4-AP (Fig. 4a curve A). The UV-vis spectra are not very irregular since the reaction proceeds rather fast, meanwhile, the reaction leads to the generation of a large amount of hydrogen, which affects the UV-vis spectra. However, the apparent rate constant of Pd-n catalysts for 4-NP reduction reaction could be assessed easily by the reduction of the intensity of the phenolate ions absorption band at 400 nm, as described in Fig. S9, and the apparent reaction rates K_{app} of Pd-n were 0.6, 0.25, 0.15 and 0.1 min^{-1}, respectively (Table S2). According to the calculated K_{app} values, Pd-1 catalyst shows much higher activity than Pd-2, Pd-3 and Pd-4 catalysts.

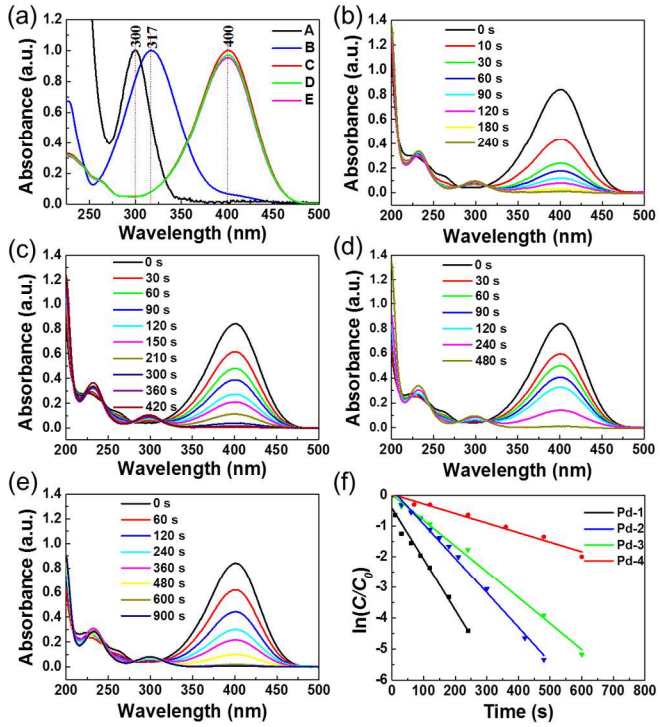

Fig. 4. (a) Normalized UV-vis spectra of 4-AP (curve A) and 4-NP in water (curve B), the addition of $NaBH_4$ in 4-NP (curve C) and after 30 min (curve D), addition of OCNTs in $NaBH_4$ and 4-NP solution (curve E); successive absorption spectra of the conversion from 4-NP to 4-AP with Pd-n catalysts: Pd-1 (b), Pd-2 (c), Pd-3 (d), Pd-4 (e); (f) plots of $\ln(C/C_0)$ versus time for the conversion from 4-NP to 4-AP with Pd-n cata-lysts.

To eliminate the effect of the hydrogen produced during the reaction in UV-vis spectra, the catalytic performances of Pd catalysts are assessed in micro-reaction vial (Method B), as shown in Fig. 4b-e, compared with Fig. 4S, two isosbestic points are observed at 280 and 312 nm. The catalytic activity tendency of Pd catalysts is consistent with that in method A, and the apparent reaction rates K_{app} of Pd-n are 1.00, 0.56, 0.50 and 0.21 min^{-1}, respectively (Table S2). Compared with method A, the precise amount of catalysts and the stir process are two main reasons for getting high K_{app}. Additionally, the catalytic activity of the Pd-5 have been investigated by 4-NP reduction reaction, the results are shown in Fig. S8. The apparent reaction rates K_{app} of Pd-5 is 0.7 min^{-1}, compared with that of Pd-n, the catalytic activity is lower than Pd-1 and a little higher than Pd-2, Pd-3 and Pd-4. It can be estimated that the presence of PdO active species is beneficial for the improvement of Pd catalytic activity. Two possible reasons can be used to explain the better catalytic activity of Pd-1. First, the complex electron interaction between the Pd and PdO component makes the H^- easy exist on the surface of Pd/PdO nanoparticles, leading to the reactive intermediates more stable. Second, the proceed of reduction reaction of 4-NP is probably more easy to on the phase boundary of Pd and PdO due to the reaction activity on the Pd surface is usually not as high as at the phase boundary of Pd and PdO component.

Usually, K_{app} is dependent on the amount of catalyst, but it is not directly related to the catalytic activity of the catalysts, whereas, the turnover frequency (TOF) is a significant parameter for evaluating the catalytic activity in heterogeneous catalytic reaction. The TOF values of various catalysts are 750, 429, 375 and 200 h^{-1} for Pd-1, Pd-2, Pd-3 and Pd-4 catalysts, respectively. In comparison with other Pd heterogeneous catalysts reported recently, such as Fe_3O_4/Pd (300 h^{-1} of TOF),[51] PEDOT-PSS-Pd (13 h^{-1} of TOF),[52] SPB/Pd (6 h^{-1} of TOF),[53] PPy/TiO_2/Pd (326 h^{-1} of TOF),[54] SBA-15/Pd (300 h^{-1} of TOF),[55] @Pd/CeO_2 (1068 h^{-1} of TOF),[56] the Pd-1 catalyst demonstrates obviously superior catalytic activity. It is clear that the Pd-1 catalyst prepared in this work is much more active than CNT/PiHP/Pd (300 h^{-1} of TOF). In addition, it is worthy to mention that the synthesis of previously reported Pd catalysts involves a multistep process, which limits their practical applications.

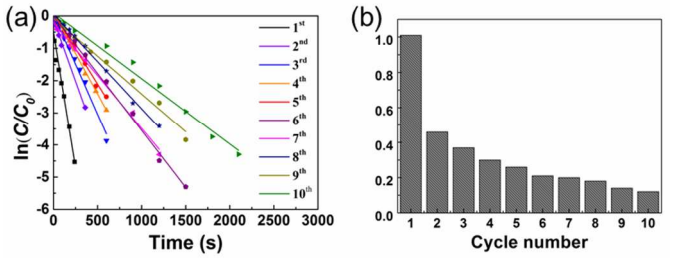

Fig. 5. (a) Plots of $\ln(C/C_0)$ versus time for 10 cycles of the conversion from 4-NP to 4-AP with Pd-1 catalyst; (b) The K_{app} of the Pd-1 during 10 cycles of the same reduction reaction.

Reusability is one of the most important features for a heterogeneous catalyst, which is better than a homogenous one. First, in order to confirm that the reaction is indeed catalyzed by solid Pd-1 rather than homogenous Pd species, leaching experiments have been carried out after the catalytic reduction of 4-NP was carried out for 1 min under standard conditions, then the supernatant was separated, and no further reaction took place after removing the catalyst. In addition, the leaching of the Pd has been also examined using ICP-OES, and no leaching of Pd was detected. To assess the recyclability of Pd-1, multiple 4-NP reduction cycles have been carried out, the Pd-1 can be repeatedly used for 10 times, and the conversion of 4-NP can be totally completed with the increase of reaction time. It is interesting to find that the catalytic activity decreased after the 1st cycle, and the conversion of 4-NP can be completed with

increasing of the reaction time from the 2nd to the 10th cycle (Fig. 5a and b), which is possibly due to the PdO active species losing during the reduction reaction after the 1th cycle reaction, this phenomenon also indicates that the existence of PdO active species in Pd-1 can greatly promote the 4-NP reduction reaction. Moreover, the TEM image of the catalyst after the reactions for 10 cycles indicates that particle size is a little bit increased, as shown in Fig. S10.

Conclusions

In summary, we have developed a facile approach for the controllable synthesis of Pd and Pd/PdO nanoparticles functionalized OCNTs by a GLIP method with different Pd salt precursors. The synthesized hybrid materials have been utilized as catalysts to study the reduction of 4-NP reaction. The results indicate that the Pd/PdO catalyst exhibit high catalytic activity compared with other Pd catalysts, which TOF value is up to 750 h^{-1}, and the current catalyst can be repeatedly used for 10 times with complete conversion of 4-NP. The catalytic activity decreased after the 1st cycle. These results confirm that the existence of PdO is the key point for the enhancement of the catalytic activity for reduction of 4-NP reactions. Further work is in progress to extend such kind of catalysts for other organic molecular transformations.

Acknowledgements

This work was supported by National Natural Science Foundation of China (Nos. 21202203, 21106184 and 21322609), the Science Foundation Research Funds Provided to New Recruitments of China University of Petroleum, Beijing (YJRC-2013-31 and Nos.YJRC-2011-18), and Thousand Talents Program.

References

1 S. Wu, J. Dzubiella, J. Kaiser, M. Drechsler, X. Guo, M. Ballauff, Y. Lu, *Angew. Chem. Int. Ed.,* 2012, **51**, 2229-2233.
2 C. Burda, X. Chen, R. Narayanan and M. A. El-Sayed, *Chem. Rev.,* 2005, **105**, 1025-1102.
3 P. Puthiaraj and K. Pitchumani, *Green Chem.*, 2014, **16**, 4223-4233.
4 G. Wei, W. Zhang, F. Wen, Y. Wang, M. Zhang, *J. Phys. Chem. C,* 2008, **112** , 10827-10832.
5 Y. Yamada, Y. Uozumi, *Tetrahedron* 2007, **63**, 8492-8498.
6 S. Domínguez-Domínguez, Á. Berenguer-Murcia, B. K. Pradhan,Á. Linares-Solano, D Cazorla-Amorós, *J Phys. Chem. C,* 2008, **112**, 3827-3834.
7 C.-B. Hwang, Y.-S. Fu, Y.-L. Lu, S.-W. Jang, P.-T. Chou, C. Wang, S. Yu, *J. Catal.,* 2000, **195**, 336-341.
8 S. Kidambi, J. Dai, J. Li, M. L Bruening, *J. Am. Chem. Soc.,* 2004, **126**, 2658-2659.
9 D. Fritsch, K. Kuhr, K. Mackenzie, F.-D. Kopinke, *Catal. Today,* 2003, **82**, 105-118.
10 H. Zhang, M. Jin, Y. Xiong, B. Lim and Y. Xia, *Acc. Chem. Res.,* 2012, **46**, 1783-1794.
11 K. Wada, K. Yano, T. Kondo, T.-A Mitsudo, *Catal. Today,* 2006, **117**, 242-247.
12 K. R. Thampi, J. Kiwi, M Grätzel, *Catal. Lett.,* 1990, **4**, 49-55.
13 C. Rossy, J. Majimel, M. T. Delapierre, E. Fouquet, F.-X Felpin, *Appl. Catal. A-Gen.,* 2014, **448**, 157-162.
14 W. Zhou, Y. Guan, D. Wang, X. Zhang, D. Liu, H. Jiang, J. Wang, X. Liu, H. Liu, S. Chen, *Chem-Asian. J.,* 2014, **9**, 1648-1654.
15 M. Korzec, P. Bartczak, A. Niemczyk, J. Szade, M. Kapkowski, P. Zenderowska, K. Balin, J. Lelątko, J. Polanski, *J. Catal.,* 2014, **313**, 1-8.
16 B. V. Devener, S. Anderson, T. Shimizu, H. Wang, J. Nabity, J. Engel, J. Yu, D. Wickham, S. Williams, *J Phys. Chem. C,* 2009, **113**, 20632-20639.
17 B. Jiang, S. Song, J. Wang, Y. Xie, W. Chu, H. Li, H. Xu, C. Tian, H. Fu, *Nano Res.*, 2014, **7**, 1280-1290.
18 N. M. Kinnunen, J. T. Hirvi, M. Suvanto, T. A. Pakkanen, *J Phys. Chem. C,* 2011, **115**, 19197-19202.
19 E. A. Karakhanov, A. L. v. Maximov, Y. Kardasheva, V. Semernina, A. Zolotukhina, A. Ivanov, G. Abbott, E. Rosenberg, V. Vinokurov, *ACS Appl. Mater. Interface,* 2014, **6**, 8807−8816.
20 S. NatháJha, *Chem. Commun.,* 2012, **48**, 8000-8002.
21 J. Mondal, T. Sen, A. Bhaumik, *Dalton Trans.,* 2012, **41**, 6173-6181.
22 U. Mandi, M. Pramanik, A. S. Roy, N. Salam, A. Bhaumik, S. M. Islam, *RSC Adv.,* 2014, **4**, 15431-15440.
23 Y. Lan, L. Yang, M. Zhang, W. Zhang, S. Wang, *ACS Appl. Mater. Interface,* 2009, **2**, 127-133.
24 Y. Shiraishi, K. Fujiwara, Y. Sugano, S. Ichikawa, T. N. Hirai, *ACS Catal.,* 2013, **3**, 312-320.
25 A. J. Hensley, Y. Hong, R. Zhang, H. Zhang, J. Sun, Y. Wang, J.-S. McEwen, *ACS Catal.,* 2014, **4**, 3381-3392.
26 H. Zhang, J. Sun, V. Lebarbier, B. Halevi, A. K. Datye, Y. Wang, *ACS Catal.,* 2014, **4**, 2379-2386.
27 A. Corma, H. Garcia and F. Llabrés i Xamena, *Chem. Rev.,* 2010, **110**, 4606-4655.
28 J. Liu, L. Chen, H. Cui, J. Zhang, L. Zhang and C.-Y. Su, *Chem. Soc. Rev.,* 2014, **43**, 6011-6061.
29 H. Li,; Z. Zhu,; F. Zhang, S. Xie, H. Li, P. Li, X. Zhou, *ACS Catal.,* 2011, **1**, 1604-1612.
30 G. G. Wildgoose, C. E. Banks and R. G. Compton, *Small*, 2006, **2**, 182-193.
31 F. Wei, Q. Zhang, W.-Z. Qian, H. Yu, Y. Wang, G.-H. Luo, G.-H. Xu, D.-Z. Wang, *Powder Technol.,* 2008, **183**, 10-20.
32 T. M. Day, P. R. Unwin, J. V. Macpherson, *Nano Lett.,* 2006, **7**, 51-57.
33 H. C. Choi, M. Shim, S. Bangsaruntip, H. Dai, *J. Am. Chem. Soc.,* 2002, **124**, 9058-9059.
34 Z. Sun, Z. Liu, B. Han, S. Miao, Z. Miao, G. An, *J. Colloid Interface Sci.,* 2006, **304**, 323-328.
35 Y. Xing, *J. Phy. Chem. B,* 2004, **108**, 19255-19259.
36 M. Cano, A. Benito, W. K. Maser, E. P. Urriolabeitia, *Carbon,* 2011, **49**, 652-658.
37 C. De Zorzi, G. Rossetto, D. Calestani, M. Zha, A. Zappettini, L. Lazzarini, M. Villani, N. E. Habra, L. Zanotti, *Cryst. Res. Technol.,* 2011, **46**, 847-851.
38 J. Keating, G. Sankar, T. I. Hyde, S. Kohara, K. Ohara, *Phys. Chem. Chem. Phys.,* 2013, **15**, 8555-8565.

39 A. Doménech-Carbó, E. Coronado, P. Díaz, A. Ribera, *Electroanal.,* 2010, **22**, 293-302.
40 D. Jose, B. R. Jagirdar, *J. Solid State Chem.,* 2010, **183**, 2059-2067.
41 W. Chu, L. N. Wang, P. A. Chernavskii, A. Y. Khodakov, *Angew. Chem. Int. Ed.,* 2008, **47**, 5052-5055.
42 J. Hong, W. Chu, P. A. Chernavskii, A. Y. Khodakov, *J. Catal.*, 2010, **273**, 9-17.
43 L. Ren, F. Yang, Y. Li, T. Liu, L. Zhang, G. Ning, Z. Liu, J. Gao and C. Xu, *RSC Adv.,* 2014, **4**, 26804-26809.
44 T. Liu, F. Yang, Y. Li, L. Ren, L. Zhang, K. Xu, X. Wang, C. Xu and J. Gao, *J. Mater. Chem. A,* 2014, **2**, 245-250.
45 F. Yang, Y. Li, T. Liu, K. Xu, L. Zhang, C. Xu and J. Gao, *Chem. Eng. J.,* 2013, **226**, 52-58.
46 T. Kaneko, K. Baba, T. Harada and R. Hatakeyama, *Plasma Processes Polym.,* 2009, **6**, 713-718.
47 O. Hofft and F. Endres, *Phys. Chem. Chem. Phys.,* 2011, **13**, 13472-13478.
48 J. Lin, T. Mei, M. Lv, C. a. Zhang, Z. Zhao, X. Wang, *RSC Adv.*, 2014, **4**, 29563-29570.
49 S. Hrapovic, E. Majid, Y. Liu, K. Male, J. H. Luong, *Anal. Chem.,* 2006, **78**, 5504-5512.
50 S. Saha, A. Pal, S. Kundu, S. Basu, T Pal, *Langmuir,* 2009, **26**, 2885-2893.
51 K. Jiang, H.-X. Zhang, Y.-Y. Yang, R. Mothes, H. Lang, W.-B. Cai, *Chem. Commun.,* 2011, **47**, 11924-11926.
52 S. Harish, J. Mathiyarasu, K. Phani, V. Yegnaraman, *Catal. Lett.,* 2009, **128**, 197-202.
53 Y. Mei, Y. Lu, F. Polzer, M. Ballauff, Drechsler, M. *Chem. Mater.,* 2007, **19**, 1062-1069.
54 X. Lu, X. Bian, G. Nie, C. Zhang, C. Wang and Y. Wei, *J. Mater. Chem.,* 2012, **22**, 12723-12730.
55 J. Morere, M. Tenorio, M. Torralvo, C. Pando, J. Renuncio, A. Cabanas, *J. Supercrit. Fluid.,* 2011, **56**, 213-222.
56 B. Liu, S. Yu, Q. Wang, W. Hu, P. Jing, Y. Liu, W. Jia, Y. L. Liu, J. Zhang, *Chem. Commun.,* 2013, **49**, 3757-3759.